Fabrication of Dynamic Holograms on Polymer Surface by Direct Laser Writing for High-Security Anti-Counterfeit Applications

JIAHAO MIAO[1], XINGHUO DING[1], SHENGJUN ZHOU[1,2], AND CHENGQUN GUI[1]

[1]Center for Photonics and Semiconductors, School of Power and Mechanical Engineering, Wuhan University, Wuhan 430072, China
[2]State Key Laboratory of Applied Optics, Changchun Institute of Optics, Fine Mechanics and Physics, Chinese Academy of Sciences, Changchun 130033, China

Corresponding author: Shengjun Zhou (zhousj@whu.edu.cn)

ABSTRACT Anti-counterfeit technology has attracted much attention with the development of economy, because many counterfeit products that are difficult for identification have been produced, which extremely damage the interests of consumers. Here, a high-resolution ultraviolet direct laser writer is applied to fabricate computer-generated holograms (CGH) with laser spot size of 300 nm for anti-counterfeit applications. The characteristics of the reconstructed images illuminated by monochromatic light are demonstrated in details. Additionally, colorful reconstructed images are observed with white light illumination in the high-security holograms samples. Furthermore, a kinematic effect of colorful reconstructed images are also observed by modifying focus depth and object size in the algorithm. The normal first (+1st) order diffraction and negative first (-1st) order diffraction in the high-security holograms exhibit different sizes due to distinguishing magnifications. The kinematic effect of white-light holograms shows great potential in anti-counterfeit applications due to its simplicity for recognition and high security since they are hard to duplicate.

INDEX TERMS Dynamic hologram, anti-counterfeit, direct laser writing.

I. INTRODUCTION

The commodity security is facing huge challenges because a large number of counterfeit products are flooded into the market, especially in alcohol and tobacco industry. In order to solve this problem, high technical barriers are needed to prevent forgery by applying complicated technology such as computer generated hologram(CGH) [1]–[7], security code [8] or barcode and periodic grating microstructures [9] so that the production of the counterfeits is much more difficult and costs more. However, security code and barcode are inconvenient for recognition as users need to verify them by specified website or devices. Also, the periodic grating microstructures take risk of being easily duplicated due to their consistent periodicity. It seems that CGH is a better solution to fabricate anti-counterfeit labels for commodity security because users can see the unique change of images

The associate editor coordinating the review of this manuscript and approving it for publication was Jingfeng Song.

and colors of each genuine product clearly depending on different viewing angles.

CGH shows great potential since it was first reported by Lohmann and Paris [10]. Theoretically, CGH needs massive calculation which could take a lot of time on hologram record, restraining its application to some extent. However, with the development of CGH, many optimization algorithms [11]–[13] such as Fast Fourier Translation (FFT) were reported to decrease the difficulty of computation and computing time. With continuous improvement of computer performance, CGH is more convenient for hologram record compared to the optical holograms [14]–[18], which does not acquire complicated optical system such as coherent light source and other optical elements. Additionally, the hologram record is accomplished by a computer, making CGH flexible for fabricating any kinds of patterns. Moreover, computer generated holographic technology could use artificial images to design holograms that could not be replaced by optical holograms. It has been reported that CGH has many

applications such as three-dimension displays [19]–[22], anti-counterfeit [24]–[27], data storage [28]–[30], etc.

Recently, Storm et al. proposed a microstructuring strategies using direct laser interference patterning (DLIP) to obtain structural colors on transparent PET-G [31]. Tamulevičius et al. proposed an dot-matrix hologram rendering algorithm based on the conical diffraction formalism and validated it by employing DLIP [32]. However, the structural colors were not visible or attractive enough to recognize and the femtosecond laser used to fabricate dot-matrix hologram by varying the fluence per pulse was expensive and not suitable for fabricating microstructures consisting of continuous lines.

Here we propose a novel dynamic hologram fabricated on polymer materials through direct laser writing (DLW) and an interesting and visible kinematic effect appears when illuminated by white light, which makes the holographic label easy for recognition. Ultraviolet DLW [33]–[38]a with continuous wave in this work was applied to fabricate micro and submicro-resolution CGH. For micro-resolution holograms, the reconstructed images were observed and their characters were demonstrated in details. For submicro-resolution holograms, it was visualized to see the kinematic effect of the reconstructed image of the holograms at the white light illumination. This kinematic effect of the reconstructed image makes the holograms more suitable for high-security applications because of its higher resolution and simplicity of recognition. In addition, this hologram consisted of several hundred millions pixels with every single pixel size of 400 nm, which made the hologram almost impossible for duplication without original template.

II. PRINCIPLE AND METHODS

Before the fabrication of the holograms, we demonstrate the principle of the hologram. To calculate the holographic data, an original xy image plane is defined to be parallel to the x_1y_1 holographic plane and both of the planes are perpendicular to the Z axis. The light field distribution $H(x_1, y_1)$ on the holographic plane is given by [39]

$$H(x_1, y_1) = \int_{-\infty}^{\infty} \int_{-\infty}^{\infty} A(x, y)e^{ikr} dxdy \qquad (1)$$

where $A(x, y)$ is the intensity distribution of the original image and $k = 2\pi/\lambda$, λ is the wavelength, and r is the distance from the point on the holographic plane to the point on the original image plane which is being calculated.

For the digital hologram calculation, the data of the original image were m × n matrix with real number and holographic data were N × N matrix with complex number. The intensity of each pixel on the hologram was the overlay of interference of all the pixels as point light source on the original image. The integral calculation at the optical hologram was replaced by summation formula at the digital hologram.

Theoretically, the hologram reconstruction is defined as [40]

$$i = coo^* + crr^* + cr^*o + cro^* \qquad (2)$$

where i is the light distribution on the screen, c, o, and r are the illuminated light wave, object light wave, and reference light wave respectively, o∗ and r∗ are the conjugate wave of object light wave and the reference light wave, respectively. The third and fourth terms of "(2)" are the description of normal first order (+1st order) diffraction and negative first order (-1st order) diffraction, respectively.

From the mathematical description of the reconstructed image, the coordinates of the reconstructed image was described as [41]

$$x_i = \frac{z_i}{z_p}x_p \pm \frac{\lambda_2}{\lambda_1}\left(\frac{z_i}{z_0}x_0 - \frac{z_i}{z_R}x_R\right) \qquad (3)$$

$$y_i = \frac{z_i}{z_p}y_p \pm \frac{\lambda_2}{\lambda_1}\left(\frac{z_i}{z_0}y_0 - \frac{z_i}{z_R}y_R\right) \qquad (4)$$

$$z_i = \left[\frac{1}{z_p} \pm \frac{\lambda_2}{\lambda_1}\left(\frac{1}{z_0} - \frac{1}{z_R}\right)\right]^{-1} \qquad (5)$$

where (x_0, y_0, z_0), (x_R, y_R, z_R), (x_p, y_p, z_p), and (x_i, y_i, z_i) are the coordinates of original image, reference light source, illuminated light source and reconstructed image, respectively. The λ_1 and λ_2 are the object wavelength and illuminated light wavelength, respectively. The sign of "±" represented the +1st order diffraction and the -1st order diffraction. From "(3)," "(4)," and "(5)", it was obvious that the coordinates of the reconstructed image exhibited linear relation with the coordinates of the illuminated light source. Additionally, the magnification of the reconstructed images was different for +1st order diffraction and -1st order diffraction, which were expressed as [41]

$$M = \left|\frac{dx_i}{dx_0}\right| = \left|\frac{dy_i}{dy_0}\right| = \left|1 - \frac{z_0}{z_R} \pm \frac{\lambda_1 z_0}{\lambda_2 z_p}\right|^{-1} \qquad (6)$$

where M is the magnification. It can be inferred from "(6)" that the size of +1st order diffraction is smaller than that of −1st order diffraction.

It is worth noting that the resulting hologram described in equation "(1)" does not take reference light into account. However, in the case of reference beam skew or vertical to the holographic plane, reference light would affect final result. Since the intensity and phase of reference light are constant at propagation direction, the phase of reference light will vary obviously across the holographic plane to affect the final light field distribution when the reference beam is not parallel to the holographic plane.

III. CALCULATION AND FABRICATION OF COMPUTER-GENERATED HOLOGRAM

The calculation is based on integration algorithm. First, a gray-scale bitmap was input into the program code and was recognized as a matrix, and each value in the matrix represented a pixel of the bitmap. All the gray-scale values of the bitmap were applied for one time integral calculation as mentioned in "(1)" and generated one output pixel data. Here, the input bitmaps contain 256 gray scale levels. In this program, we were supposed to set the number of
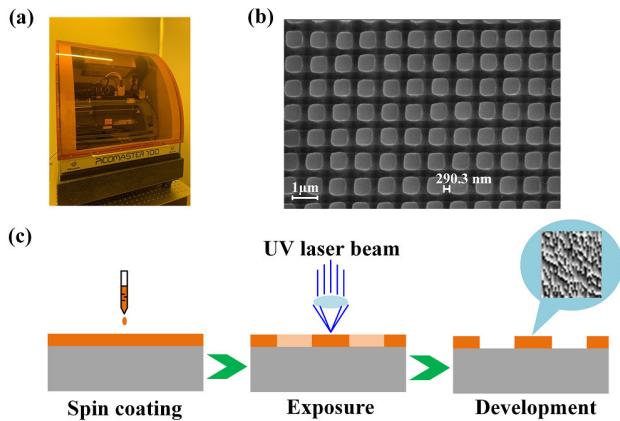
FIGURE 1. (a) Image of PicoMaster 100 direct laser writer. (b) SEM Image of micro-structure fabricated by direct laser writer. (c) Schematic illustration of fabrication procedure of hologram on polymer surface. The DLW procedure functioned as step "exposure", which was similar to conventional lithography except without mask.

FIGURE 2. Schematic illustration of the hologram reconstruction. As laser propagates through the hologram, the microstructure on the hologram forms new light source according to Huyghens principle. Finally, the new light source interferes with each other and generates the pattern we have designed.

output pixels, resolution and focus depth, respectively. Here, the focus depth defined the distance between hologram and screen for reconstruction. It is noted that the diffraction angles increased as the resolution improved. For micro-resolution hologram, the resolution and focus depth were set to be 2 μm and 1 m respectively. The long focus which was 1 m in this work only needed shallow diffraction angles, indicating that the hologram did not require high resolution. The number of output pixels are 2000×2000 that would take 4 million times of the integral calculations. For the kinematic hologram, the resolution and focus depth were designed to be 200 nm and 0.003 m, respectively. This short focus depth needed high diffraction angles which require high resolution to accurately describe the frequency information of wavefront. The number of the output pixels are 25000×25000, which would take 625 million times of the integral calculations. The computation time depends on the numbers of output pixels and numbers of gray-scale values from input bitmap.

We applied ultraviolet DLW to fabricate the CGH. The direct laser writer (PicoMaster 100) was manufactured by 4PICO B.V in Netherland as shown in Fig. 1a. This DLW system uses a 405 nm wavelength of continuous wave laser as exposure source, with a Gaussian lateral intensity distribution that reaches 300 nm of FWHM value. The numerical aperture is 0.85 and the exposure strategy is single spot. Here, 300 nm of FWHM of laser determines spot size to be 300nm. However, as shown in Fig. 1b, we can achieve higher resolution by changing the distance between two spots, which are correlated with stepping distance. The laser beam is highly focused by lens on the surface of workpiece, and the rasterizing principle of the machine ensures proper and constant exposure over the whole surface, scanning the substrate at high speed and stepping the laser head with a software adjustable pitch to write the lines as designed. There was a threshold value to control the DLW process and the holographic data under the threshold value would be exposed.
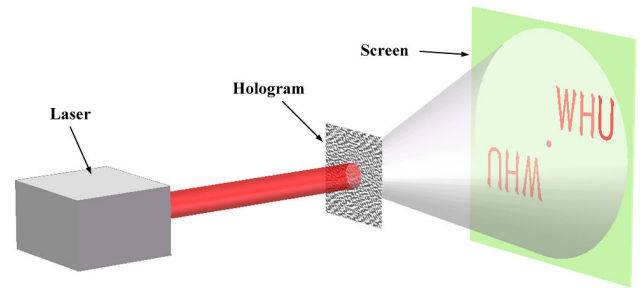
The fabrication procedure of CGH is shown in Figure 1c, which was familiar with conventional mask lithography [42]–[44]. First, a glass substrate was cleaned with acetone and ethyl alcohol. 2.2-μm-thick positive photoresist (S1818, Microposit) was then coated on the glass substrate by spin coater. The speed of the spin coater was 600 r/min for 20 seconds and then switched to 3000 r/min for 100 seconds. After that, the glass substrate was put onto hot plate to bake for 2 minutes with temperature of 90 °C. The recording temperature was 21 °C. During the exposure process, position of laser spot in scanning direction and stepping direction were controlled by linear motor and voice coil motor, respectively. The stepping distance and scanning speed were set to be 150 nm and 200 mm/s, respectively. The scanning frequency and scanning resolution were 10 MHz and 20 nm, respectively. Stepping motion and scanning motion performed alternatively. Additionally, the laser density was set to be 600 mJ/cm^2. Finally, the substrate was dipped into the positive photoresist developer (FUJIFILM Electronic Materials U.S.A. Inc.,) for 20 seconds and then deionized water was applied to clean the polymer surface applied with holographic microstructure. After all the procedures, a binary digital hologram was fabricated. The hologram could be more visible after metallization by evaporating nickel on the surface of the hologram. The microstructures were observed by optical microscope (DM3 XL, LEICA Microsystems CMS GmbH).

IV. RESULTS AND DISCUSSION

Figure 2 shows schematic illustration of the hologram reconstruction. The hologram was illuminated vertically to its plane by the same wavelength laser that was defined in the holographic calculation process. The laser functioned as reference beam. Due to the existence of microstructure on surface of substrate, the pixels being exposed on the hologram formed new light source and exhibited diffraction and interference with each other. Finally, the pattern diffracted from hologram could be seen without lens on the screen as shown in Fig. 2, which was consistent with the original image. The schematic diagram shows the zero order (0th order)
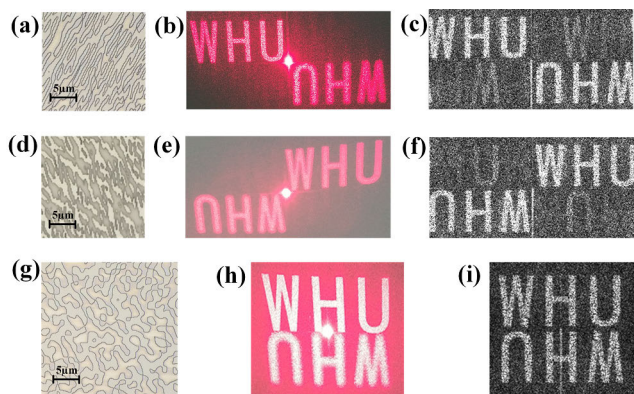
FIGURE 3. Holograms, reconstructed images and simulation results. The sizes of reconstructed image are changeable, which depend on the distance between hologram and screen. (a) (d) (g) Optical microscope of holograms. (b) (e) (h) Reconstructed image illuminated by red laser (630 nm). The reconstructed images showed that -1st order diffraction looked fuzzy because of the aberration. (c) (f) (i) MATLAB simulation results of hologram. The results were consistent with the experimental reconstructed images.
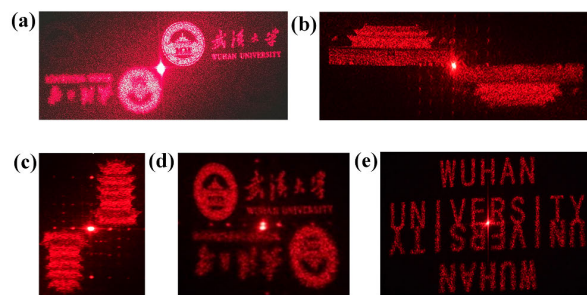

FIGURE 4. Five reconstructed images illuminated by red laser (630 nm). The sizes of reconstructed image are changeable, which depend on the distance between hologram and screen. (a) (d) Logo of Wuhan University. (b) Image of Tian An Men. (c) Image of Yellow Crane Tower in Wuhan. (e) Capital letters of Wuhan University. All the reconstructed images had the same character that the +1st order diffraction looked clear but the -1st order looked fuzzy.

diffraction, +1st order diffraction and -1st order diffraction of the pattern of ''WHU.''

The hologram fabricated by DLW and the reconstructed image are shown in Fig. 3. Figure 3a shows the optical microscope image of hologram sample fabricated by DLW using hologram data from analog hologram of pattern ''WHU'' generated by the computer program, which was capable of simulating the hologram reconstruction. The simulated results from MATLAB software was consistent with the experimental hologram reconstruction illuminated by red laser (630 nm), which are shown in Figs. 3b and c, respectively. The size of the hologram was 2 mm × 2 mm with the resolution of 2 μm, revealing that the hologram consisted of 1000 × 1000 pixels. In addition, the hologram does not need other optical elements for reconstructed image, which is easy for hologram reconstruction and suitable for anti-counterfeit applications.

To get a better understanding of the hologram, we demonstrated more details of hologram and its reconstructed image. Figures 3d e, f and g, h, i shows the hologram, reconstructed image and simulation image, respectively. Additionally, the direction of 0th order diffraction, +1st order diffraction and −1st order diffraction as shown in Fig. 3b were perpendicular to the direction of the small pattern in the hologram in Fig. 3a. For example, the direction of +1st, 0th, and −1st order diffraction in Fig. 3b was from upper left to low right, which is contrary to the direction of the micromorphological pattern in the hologram in Fig. 3a from lower left to upper right. This character was also confirmed by Figs. 3d and Fig. 3e, which were also perpendicular to each other.

More importantly, the −1st order diffraction looks fuzzy as shown in Figs. 3b, e, and h, which was caused by aberration. When the illuminated light wave is equal to reference light wave, the third term of ''(2)'' is equal to $rr*o$, which is a

perfect reconstruction of the object light wave because $rr*$ is constant that would not affect the object light wave. However, the fourth term of ''(2)'' is $rro*$ from which the coefficient rr is not constant, which is the main reason causing aberration on the conjugate light wave. The −1st order diffraction looks fuzzy because that conjugate image overlaps with reconstructed image. Additionally, the second term of ''(2)'' are zero order diffraction, which is a bright spot at the center of reconstructed image. The first term of ''(2)'' represents noise and cannot be eliminated.

More samples were fabricated to verify the fuzzy phenomenon of -1st order diffraction. Figure 4 shows the reconstructed images of five samples illuminated by red laser. The logo of Wuhan University was exhibited in Fig. 4a and d. Figure 4b and c show the reconstructed images of Tian An Men which is in Beijing and Yellow Crane Tower that is in Wuhan, respectively. Figure 4e depicts the pattern of ''WUHAN UNIVERSITY.'' These five samples had common characters that the -1st order diffraction looked fuzzy due to the aberration that was demonstrated above. In addition, the aberration looked more obvious in the five samples than the pattern of ''WHU'' because the object light wave of these five samples were more complicated than the pattern of ''WHU,'' which made the aberration play a more important role in the −1st order diffraction of reconstructed images.

Despite of the fuzzy of the −1st order diffraction, another important character of the hologram was demonstrated. It should be noted that each point of the hologram was the interference results of both object light wave and reference light wave, which means that a small part of the hologram included all the information of the object light wave to show the entire reconstructed image. So theoretically, every small part of the hologram could be used for hologram reconstruction with laser illumination. Figure 5a shows schematic illustration of a synthesized hologram consisting of two different holograms. Here the two different holograms with size of 2 mm × 2 mm were divided into four parts where every area was 1 mm × 1 mm. Then, the area A and D in hologram I and the area F and G in hologram II were combined
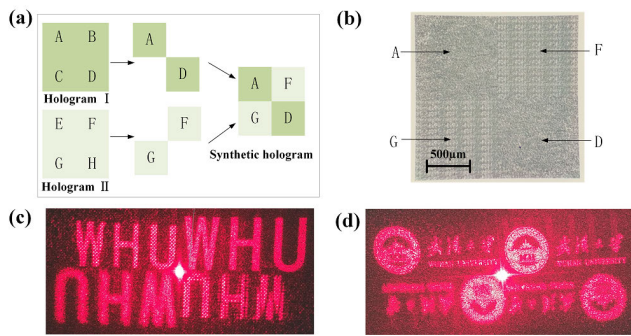
FIGURE 5. Schematic illustration of synthesized hologram and its reconstructed images. The sizes of the reconstructed images are changeable, which depend on the distance between hologram and screen. (a) Schematic diagram of the synthesized hologram. (b) Optical microscope of synthesized hologram. (c)-(d) Reconstructed images of two synthesized hologram. The results indicated that a small part of the hologram contained all the information of the objected light wave.
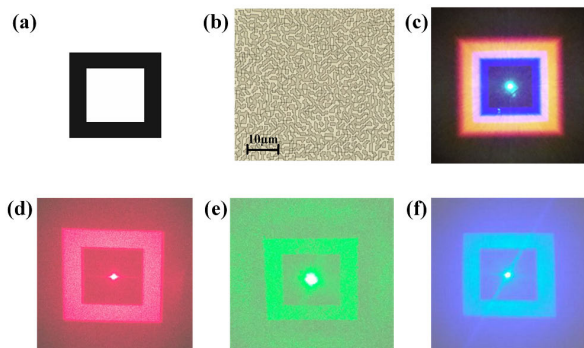

FIGURE 6. Holograms and reconstructed images illuminated by monochromatic light and white light. The sizes of the reconstructed images are changeable, which depend on the distance between hologram and screen. (a) Original image used for computer-generated hologram. (b) Optical microscope image of hologram sample fabricated by DLW. (c) Colorful reconstructed image illuminated by white light. Reconstructed image illuminated by (d) red laser (630 nm), (e) green laser (530 nm) and (f) blue laser (452 nm), respectively. The presence of the colorful reconstructed image indicated that the position of the reconstructed images shows linear relation with wavelength of the illuminated light.

to form the synthesized hologram as shown in Fig. 5a. Figure 5b shows the optical microscope of synthesized hologram fabricated by DLW. Fig 5c and d show four reconstructed images that were diffracted from the synthesized holograms. In Figure 5c, the bigger "WHU" from lower left to upper right was generated from Hologram I, and smaller "WHU" was generated from Hologram II, as shown in Fig 5a. The same case was applied in Fig 5d. Both images could be seen on the screen at once, which confirmed that a part of the hologram contained all the information of the objected light wave and could be used for hologram reconstruction.

The hologram reconstruction illuminated by white light was presented in Fig. 6. The original pattern, optical microscope image of hologram and the reconstructed image of the hologram illuminated by white light were shown in Figs. 6a, b, and c, respectively. Figure 6d, e, and f show the reconstructed images illuminated by red laser (630 nm),

green laser (530 nm) and blue laser (452 nm), respectively. Compared with single laser illumination, a colorful reconstructed image was observed by white light illumination as mentioned in Fig. 6c. In order to obtain clear and colorful reconstructed image, optical lens was essential for focus imaging in white-light hologram reconstruction. The better way was putting a camera behind the hologram replacing the screen as we did in Fig. 5c to observe the colorful reconstructed images. According to equation "(3)"–"(5)", the coordinates of the reconstructed image exhibited linear relation with the coordinates of the illuminated light source and were related to the wavelength of illuminated light. The result of colorful reconstructed image indicated that white light were separated into several monochromatic light and diffracting to form the reconstructed image at different position because of the different wavelength. Moreover, the size of the reconstructed image in every single color in Fig. 6c was dependent on variation of wavelength and the size became larger as the wavelength increased, indicating that the +1st order diffraction was far away from the 0th order diffraction as wavelength increased.

For the colorful reconstructed image illuminated by white light, other samples were fabricated to observe the colorful reconstructed images, as shown in Fig. 7. It was obvious to observe the rainbow color of the reconstructed images of the pattern with "WHU" in Figs. 7b, c, and d. The rainbow effect appeared difference between Figs. 7b and 6d, which was due to the different resolution of the holograms where the resolutions of Figs. 7b and d were 1 um and 2 um, respectively. In addition, the reconstructed images in Figs. 7b and d were illuminated by different white light sources, which could be recognized by the different diffracted color in reconstructed images. The spectra of these two white light sources were shown in Fig. 7e. Holograms of Fig. 7a and b were illuminated by white light I, and holograms of Fig. 7c and d were illuminated by white light II. The relative intensity of blue light in the spectrum of white light I was much larger than that of blue light in the spectrum of white light II, resulting in that diffracted color in Fig. 7c and d presented more blue areas than in Fig. 7a and b. This phenomenon shows great potential application for analyzing composition of various light sources. However, the rainbow effect made the reconstructed images look fuzzy especially when the original image was complicated such as the logo of Wuhan University of which the rainbow reconstructed image was shown in Fig. 7a. Here, the hologram of the logo of Wuhan University contained 25000 × 25000 pixels, and hologram of the pattern of "WHU" contained 2000 × 2000 pixels. We observed that the pattern near the 0th order diffraction became highlight, because the monochromatic light diffraction overlaid with each other forming the white light.

In order to eliminate the optical lens especially the camera to simplify the hologram reconstruction process illuminated by white light, a hologram with small focus depth was fabricated by DLW. Figure 8a shows the scanning electronic microscope of the hologram with resolution of 400 nm.
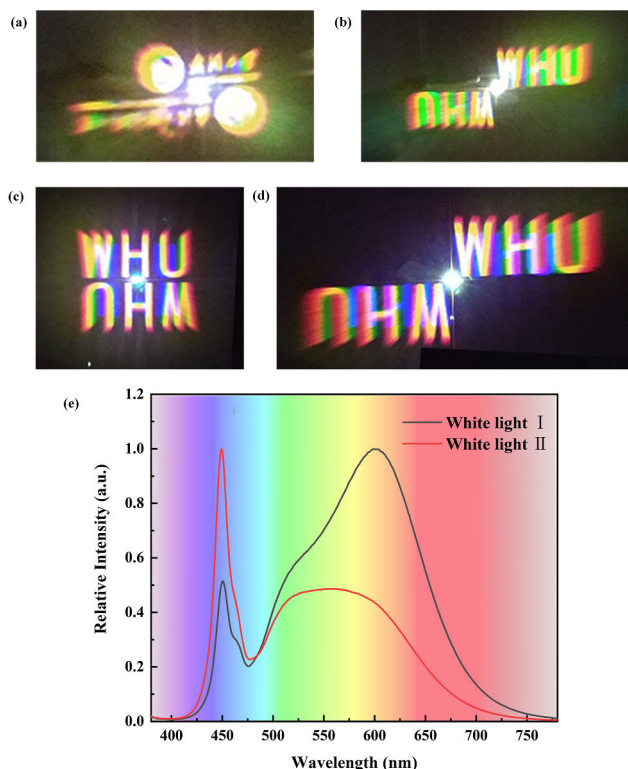
FIGURE 7. Rainbow reconstructed images of four hologram samples and spectra of two different white light sources. The sizes of reconstructed image are changeable, which depend on the distance between hologram and screen. (a) The rainbow effect made the reconstructed images look fuzzy especially when the original image contained too much information such as the logo of Wuhan University. (b) Colorful reconstructed image illuminated by the same white light with the logo of Wuhan University. (c)-(d) Two different reconstructed images of the pattern of "WHU" illuminated by the same white light. The illuminated white light used in (a) and (b) was different from the illuminated white light used in (c) and (d), which was shown in (e).

Figure 8b, c, and d show the reconstructed image illuminated by white light, red laser (630 nm), and green laser (530 nm), respectively. The size of the circular holograms shown in Fig. 8b is 10 mm × 10 mm. We found that the diffracted pattern moved consistently as we changed the position of the illuminated light. This observation can be explained by "(3)," "(4)," and "(5)." As shown in Figs. 8b, c, and d, the diffracted patterns of "PS" appeared at different position in the hologram as we moved the illuminated light around the sample.

In addition, the size of the +1st order diffraction and −1st order diffraction shows reverse change as we moved the illuminated light close to the hologram along the axis direction due to the difference of magnification as mentioned in "(6)." Moreover, the −1st order diffraction was always larger than the +1st order diffraction because the magnification of −1st order diffraction was larger than that of +1st order diffraction, which was consistent with "(6)." However, as we moved the illuminated light far away from the hologram, the sizes of the +1st order diffraction and the −1st order diffraction were almost the same, because the spherical wave
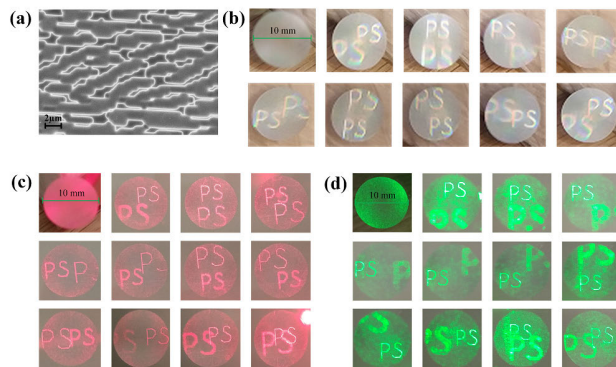

FIGURE 8. Microstructure of the hologram and reconstructed image illuminated by white light, red laser (630 nm) and green laser (530 nm). The size of hologram is 10 mm × 10 mm. (a) SEM image of hologram. (b) The colorful reconstructed image moved consistently as we move the position of the illuminated light. (c) Reconstructed image at different position illuminated by red laser. (d) Reconstructed image at different position illuminated by green laser.
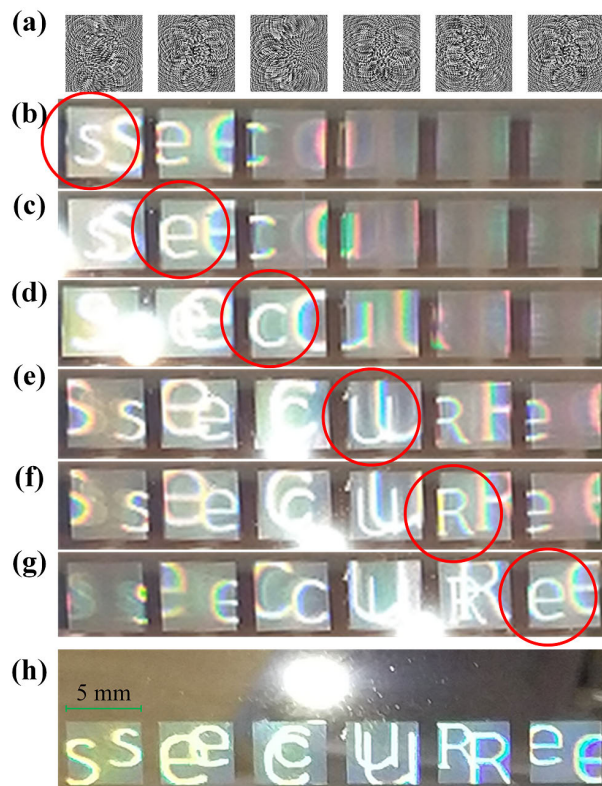

FIGURE 9. Six holograms and their reconstructed images arranged in line. The sizes of each hologram is 5 mm × 5 mm. Each reconstructed image appeared and disappeared when the light source moved from left to the right, horizontally. (a) Six light intensity distribution holograms with pattern of "secuRe" generated from MATLAB software. (b)-(g) The pattern of "secuRe" appeared and then disappeared one by one as marked red. (h) The big white spot as light source behind the glass substrate. With the white spot illumination in the center, six reconstructed image appeared and formed the word "secuRe."

generated from the light source could be regarded as plane wave when the light source was far away from the hologram. This phenomenon could also be demonstrated from "(6)."

When the illuminated light was far away from the hologram, Z_p was much larger than Z_0, which made the magnification of the +1st order diffraction approximately equal to the magnification of −1st order diffraction.

The kinematic effect in hologram illuminated by white light shows great potential for anti-counterfeit application due to its simplicity of recognition. The small flashlight used in cellphone could be a perfect light source for hologram reconstruction. Figure 9 shows six kinematic holograms arranged in line. The total size of each hologram is 5 mm × 5 mm. Six light intensity distribution holograms generated from MATLAB software were shown in Fig. 9a. As we moved white light from left to the right horizontally, the pattern of "secuRe" appeared and then disappeared one letter by one, which were marked in red from Fig. 9b to 9g. When the white light moved to the center above six holograms as shown in Fig. 9h, six reconstructed image became visible and formed secure pattern. Moreover, +1st order diffraction and -1st order diffraction in every hologram were in line with the white light source. Additionally, the results also confirm that the -1st order diffraction looks fuzzy and the size of +1st order diffraction is smaller than that of -1st order diffraction. Figure 9 was associated with a video which could be seen in "Visualization 1" in the supplementary materials. The video was recorded by camera in the cellphone with flashlight open.

V. CONCLUSION

An ultraviolet DLW was applied to fabricate micro-resolution and submicro-resolution computer-generated holograms for anti-counterfeit applications. From the results we have observed that simulated images were consistent with experimental results. Negative first order diffraction in the reconstructed image looked fuzzy because of aberration, and this aberration could be more obvious when original image was complicated. In addition, colorful reconstructed image illuminated by white light was discussed, and the position of reconstructed image shows linear relation with the wavelength of illuminated light because the white light consists of several monochromatic light. Finally, a kinematic hologram was fabricated and analyzed, kinematic effect of reconstructed image and difference of magnification between normal first order diffraction and negative first order diffraction were theoretically analyzed and confirmed by experiment. The kinematic hologram was associated with a video which could be seen in "Visualization 1" in the supplementary materials. The characteristics of low cost, difficulty to duplicate, visible and attractive kinematic effect of reconstructed image, and simplicity for recognition made the hologram exhibited great potential in anti-counterfeit applications.

REFERENCES

[1] X. Ni, A. V. Kildishev, and V. M. Shalaev, "Metasurface holograms for visible light," *Nature Commun.*, Nov. 2013, Art. no. 2807.

[2] E. Almeida, O. Bitton, and Y. Prior, "Nonlinear metamaterials for holography," *Nature Commun.*, vol. 7, Aug. 2016, Art. no. 12533.

[3] L. Li, T. J. Cui, W. Ji, S. Liu, J. Ding, X. Wan, Y. B. Li, M. Jiang, C.-W. Qiu, and S. Zhang, "Electromagnetic reprogrammable coding-metasurface holograms," *Nature Commun.*, vol. 8, no. 1, Aug. 2017, Art. no. 197.

[4] H.-C. Liu, B. Yang, Q. Guo, J. Shi, C. Guan, G. Zheng, H. Mühlenbernd, G. Li, T. Zentgraf, and S. Zhang, "Single-pixel computational ghost imaging with helicity-dependent metasurface hologram," *Appl. Opt.*, vol. 3, no. 9, Sep. 2017, Art. no. e1701477.

[5] G. Ruffato, R. Rossi, M. Massari, E. Mafakheri, P. Capaldo, and F. Romanato, "Design, fabrication and characterization of computer generated holograms for anti-counterfeiting applications using OAM beams as light decoders," *Sci. Rep.*, vol. 7, no. 1, Dec. 2017, Art. no. 18011.

[6] W. Wan, J. Gao, and X. Yang, "Metasurface holograms for holographic imaging," *Adv. Opt. Mater.*, vol. 5, no. 21, Nov. 2017, Art. no. 1700541.

[7] J. Zhang, N. Pégard, J. Zhong, H. Adesnik, and L. Waller, "3D computer-generated holography by non-convex optimization," *Optica*, vol. 4, no. 10, pp. 1306–1313, Oct. 2017.

[8] T. Vaish and M. K. Kannembath, "System and method for providing a security code," U.S. Patent 0 122 331 A1, May 1, 2014.

[9] F. Rößler, T. Kunze, and A. F. Lasagni, "Fabrication of diffraction based security elements using direct laser interference patterning," *J. Opt. Express*, vol. 25, no. 19, pp. 22959–22970, 2017.

[10] A. W. Lohmann and D. P. Paris, "Binary fraunhofer holograms, generated by computer," *Appl. Opt.*, vol. 6, no. 10, pp. 1739–1748, Oct. 1967.

[11] R. G. Dorsch, A. W. Lohmann, and S. Sinzinger, "Fresnel ping-pong algorithm for two-plane computer-generated hologram display," *Appl. Opt.*, vol. 33, no. 5, pp. 869–875, Feb. 1994.

[12] M. Makowski, M. Sypek, A. Kolodziejczyk, and G. Mikula, "Three-plane phase-only computer hologram generated with iterative Fresnel algorithm," *Proc. SPIE*, vol. 44, no. 12, Dec. 2005, Art. no. 125805.

[13] T. Shimobaba, T. Ito, N. Masuda, Y. Ichihashi, and N. Takada, "Fast calculation of computer-generated-hologram on AMD HD5000 series GPU and OpenCL," *Opt. Express*, vol. 18, no. 10, pp. 9955–9960, 2010.

[14] L. Huang, X. Chen, H. Mühlenbernd, H. Zhang, S. Chen, B. Bai, Q. Tan, G. Jin, K.-W. Cheah, C.-W. Qiu, J. Li, T. Zentgraf, and S. Zhang, "Three-dimensional optical holography using a plasmonic metasurface," *Nature Commun.*, vol. 4, Nov. 2013, Art. no. 2808.

[15] P. W. M. Tsang, J.-P. Liu, and T.-C. Poon, "Compressive optical scanning holography," *Optica*, vol. 2, no. 5, pp. 476–483, May 2015.

[16] T. Leportier, M. C. Park, Y. S. Kim, and T. Kim, "Converting optical scanning holograms of real objects to binary Fourier holograms using an iterative direct binary search algorithm," *Opt. Express*, vol. 23, no. 3, pp. 3403–3411, Feb. 2015.

[17] Y. Kobayashi and J. Abe, "Real-time dynamic hologram of a 3D object with fast photochromic molecules," *Adv. Opt. Mater.*, vol. 4, no. 9, pp. 1354–1357, Sep. 2016.

[18] S. Mukherjee, A. Vijayakumar, M. Kumar, and J. Rosen, "3D imaging through scatterers with interferenceless optical system," *Sci. Rep.*, vol. 8, no. 1, Jan. 2018, Art. no. 1134.

[19] Y. S. Kim, T. Kim, T.-C. Poon, and J. T. Kim, "Three-dimensional display of a horizontal-parallax-only hologram," *Appl. Opt.*, vol. 50, no. 7, pp. B81–B87, Mar. 2011.

[20] J. Geng, "Three-dimensional display technologies," *Adv. Opt. Photon.*, vol. 5, no. 4, pp. 456–535, Dec. 2013.

[21] H. Sasaki, K. Yamamoto, K. Wakunami, Y. Ichihashi, R. Oi, and T. Senoh, "Large size three-dimensional video by electronic holography using multiple spatial light modulators," *Sci. Rep.*, vol. 4, Aug. 2014, Art. no. 6177.

[22] O. Hernandez, E. Papagiakoumou, D. Tanese, K. Fidelin, C. Wyart, and V. Emiliani, "Three-dimensional spatiotemporal focusing of holographic patterns," *Nature Commun.*, vol. 7, Jun. 2016, Art. no. 11928.

[23] V. J. Cadarso, S. Chosson, K. Sidler, R. D. Hersch, and J. Brugger, "High-resolution 1D moirés as counterfeit security features," *Light-Sci. Appl.*, vol. 2, Jul. 2013, Art. no. e86.

[24] M. You, J. Zhong, Y. Hong, Z. Duan, M. Lin, and F. Xu, "Inkjet printing of upconversion nanoparticles for anti-counterfeit applications," *Nanoscale*, vol. 7, no. 10, pp. 4423–4431, Jan. 2015.

[25] I.-Y. Park, S. Ahn, Y. Kim, H. S. Bae, H. S. Kang, J. Yoo, and J. Noh, "Serial number coding and decoding by laser interference direct patterning on the original product surface for anti-counterfeiting," *Opt. Express*, vol. 25, no. 13, pp. 14644–14653, Jun. 2017.

[26] H. Nam, K. Song, D. Ha, and T. Kim, "Inkjet printing based mono-layered photonic crystal patterning for anti-counterfeiting structural colors," *Sci. Rep.*, vol. 6, Aug. 2016, Art. no. 30885.

[27] X. Liu, Y. Wang, X. Li, Z. Yi, R. Deng, L. Liang, X. Xie, D. T. B. Loong, S. Song, D. Fan, A. H. All, H. Zhang, L. Huang, and X. Liu, "Binary temporal upconversion codes of Mn^{2+}-activated nanoparticles for multilevel anti-counterfeiting," *Nature Commun.*, vol. 8, no. 1, Oct. 2017, Art. no. 899.

[28] T. Nobukawa, Y. Wani, and T. Nomura, "Multiplexed recording with uncorrelated computer-generated reference patterns in coaxial holographic data storage," *Opt. Lett.*, vol. 40, no. 10, pp. 2161–2164, May 2015.

[29] T. Nobukawa and T. Nomura, "Multilevel recording of complex amplitude data pages in a holographic data storage system using digital holography," *Opt. Express*, vol. 24, no. 18, pp. 21001–21011, Sep. 2016.

[30] V. Pramitha, B. Das, J. Joseph, R. Joseph, K. Sreekumar, and C. S. Kartha, "High efficiency panchromatic photopolymer recording material for holographic data storage systems," *Opt. Mater.*, vol. 52, pp. 212–218, Feb. 2016.

[31] S. Storm, S. Alamri, M. Soldera, T. Kunze, and A. F. Lasagni, "How to tailor structural colors for extended visibility and white light generation employing direct laser interference patterning," *Macromol. Chem. Phys.*, vol. 220, no. 13, Jul. 2019, Art. no. 1900205.

[32] T. Tamulevičius, M. Juodenas, T. Klinavicius, A. Paulauskas, K. Jankauskas, A. Ostreika, A. Žutautas, and S. Tamulevičius, "Dot-matrix hologram rendering algorithm and its validation through direct laser interference patterning," *Sci. Rep.*, vol. 8, no. 1, Sep. 2018, Art. no. 14245.

[33] L. B. Fletcher, J. J. Witcher, N. Troy, S. T. Reis, R. K. Brow, and D. M. Krol, "Direct femtosecond laser waveguide writing inside zinc phosphate glass," *Opt. Express*, vol. 19, no. 9, pp. 7929–7936, Apr. 2011.

[34] D. Lee, D. Paeng, H. K. Park, and C. P. Grigoropoulos, "Vacuum-free, maskless patterning of Ni electrodes by laser reductive sintering of NiO nanoparticle ink and its application to transparent conductors," *ACS Nano*, vol. 8, no. 10, pp. 9807–9814, Aug. 2014.

[35] Y. Jia, C. Cheng, J. R. Vázquez de Aldana, and F. Chen, "Three-dimensional waveguide splitters inscribed in Nd:YAG by femtosecond laser writing: Realization and laser emission," *J. Lightw. Technol.*, vol. 34, no. 4, pp. 1328–1332, Feb. 15, 2016.

[36] A. Patel, Y. Svirko, C. Durfee, and P. G. Kazansky, "Direct writing with tilted-front femtosecond pulses," *Sci. Rep.*, vol. 7, no. 1, Oct. 2017, Art. no. 12928.

[37] M. Chanal, V. Y. Fedorov, M. Chambonneau, R. Clady, S. Tzortzakis, and D. Grojo, "Crossing the threshold of ultrafast laser writing in bulk silicon," *Nature Commun.*, vol. 8, no. 1, Oct. 2017, Art. no. 773.

[38] C. Zhang, M. Gao, D. Wang, J. Yin, and X. Zeng, "Relationship between pool characteristic and weld porosity in laser arc hybrid welding of AA6082 aluminum alloy," *J. Mater. Process. Technol.*, vol. 240, pp. 217–222, Feb. 2017.

[39] N. Takai and Y. Mifune, "Digital watermarking by a holographic technique," *Appl. Opt.*, vol. 41, no. 5, pp. 865–873, Feb. 2002.

[40] R. W. Meier, "Magnification and third-order aberrations in holography," *J. Opt. Soc. Amer.*, vol. 55, no. 8, pp. 987–992, 1965.

[41] J. W. Goodman, *Introduction to Fourier optics*. Arapahoe, CO, USA: Roberts and Company, 2005.

[42] S. Zhou, H. Xu, H. Hu, C. Gui, and S. Liu, "High quality GaN buffer layer by isoelectronic doping and its application to 365 nm InGaN/AlGaN ultraviolet light-emitting diodes," *Appl. Surf. Sci.*, vol. 471, pp. 231–238, Mar. 2019.

[43] S. Zhou, X. Liu, H. Yan, Z. Chen, Y. Liu, and S. Liu, "Highly efficient GaN-based high-power flip-chip light-emitting diodes," *Opt. Express*, vol. 27, no. 12, pp. A669–A692, Jun. 2019.

[44] B. Tan, J. Miao, Y. Liu, H. Wan, N. Li, S. Zhou, and C. Gui, "Enhanced light extraction of flip-chip mini-LEDs with prism-structured sidewall," *Nanomaterials*, vol. 9, Feb. 2019, Art. no. 319.

JIAHAO MIAO is currently pursuing the master's degree with the School of Power and Mechanical Engineering, Wuhan University. His research interest includes direct laser writing with applications in electronic and photonic devices.
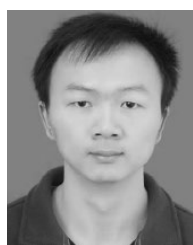
XINGHUO DING received the master's degree from the School of Power and Mechanical Engineering, Wuhan University. His research interest includes direct laser writing with applications in electronic and photonic devices.

SHENGJUN ZHOU was a Research Fellow with University of Michigan, Ann Arbor, from 2014 to 2015. He is well known as an Industrial Technologist. He has published more than 50 articles and holds ten patents. He is currently an Associate Professor with the School of Power and Mechanical Engineering, Wuhan University. His current research interests include the areas of GaN-based blue/green/ultraviolet LEDs, nitride semiconductors, nanoimprint lithography, and direct laser writing with applications in electronic and photonic devices. He has served as a Committee Member for many conferences. He is also the Co-chair of the Organizing Committee of the IEEE ICEPT 2016 Conference.

CHENGQUN GUI received the Ph.D. degree from Universiteit Twente, The Netherlands. He is currently a Professor with the School of Power and Mechanical Engineering and the Institute of Technological Sciences, Wuhan University. His current research interests include opto-mechatronics equipment, flexible electronics manufacturing, and laser micro–nano manufacturing.

• • •